RSC Advances

ROYAL SOCIETY OF CHEMISTRY

www.rsc.org/advances

Journal Name

ARTICLE

Proximal environment controlling the reactivity between inorganic sulfide and heme-peptide model

Received 00th January 20xx,
Accepted 00th January 20xx

DOI: 10.1039/x0xx00000x

www.rsc.org/

Zijian Zhao,[ab†] Dandan Wang,[a†] Mingyang Wang,[c] Xiaoli Sun[b], Liping Wang,[c] Xuri Huang,[b] Li Ma,[ad*] Zhengqiang Li[a*]

In order to extent the comprehension of the binding between inorganic sulfide and heme-containing proteins, we have synthesized a series of deuterohemin-His-peptides (DhHPs) referred to the active centers of cytochrome *c* as heme models to investigate the effects of the proximal environment on the reactivity when lack of distal residues. DhHPs contain synthetic peptides with 2, 3, 4, 5, and 6 amino acids respectively, while the imidazole side chain of His2 serves as the fifth ligand for all ferric centers. The coordination of sulfide to the ferric iron has been confirmed by UV-Vis and EPR spectroscopic studies and the kinetic constants of the binding reaction determined using a stopped-flow technique. Deuterohemin-AlaHisThrValGluLys (DhHP-6) exhibits an association rate constant k_{on} = 2.34 ×10^4 $M^{-1}s^{-1}$ that is 4-times faster than that of Deuterohemin-AlaHis (DhHP-2). While the k_{off} values of all DhHPs are close and independent of the lengths and sequences of the peptides. It is hypothesized that proximal environment plays an important role in the association processes, in which H-bond network provided by proximal polar residues may facilitate the reaction. Moreover, the existence of Glu induces an substantial increase of k_{on} in DhHP-5 and -6, indicating that the introduction of Glu5 enhances the reactivity of sulfide towards ferric centers. We have also prepared a derivative Deuterohemin-β-Ala-β-Ala-Thr-Val-Glu-Lys (DhAP-6) with Ala2 replacing His2. The results show that sulfide does not coordinate with the ferric center in DhAP-6, but reduces it to ferrous.

Introduction

Hydrogen sulfide (H_2S) is traditionally recognized as a toxic gas with a broad-spectrum of toxic effects,[1] the primary mechanism for the toxic action of H_2S is direct inhibition of cytochrome oxidase.[2] In addition, inhalation of hydrogen sulfide leads to cytotoxic damage to the nasal and pulmonary epithelium.[3] Recently, the discovery of the endogenous H_2S has dramatically changed the reputation of this gas from a toxic pollutant to a biologically relevant molecule.[4-7] H_2S is now considered to be an important neuromodulator and neuroprotector with diverse significant therapeutic potentials, including regulating synaptic transmission in neurons by enhancing the activity of the N-methyl-D-aspartate (NMDA) receptor and ATP-sensitive potassium (K_{ATP}) channels.[8-11] Remarkably, heme-containing proteins are recognized as the popular hydrogen sulfide biochemical targets. Similar to CO [12,13] and O_2,[14,15] H_2S is considered to be the third gas molecular as heme ligand. Previous studies reveal that distal heme pocket environment mainly contributes to the affinity and stability of the H_2S towards sulfide-reactive hemoglobins. For instance, HbI expressed by *Lucina pectinata* and *Vitreoscilla* hemoglobin (VHb) expressed by *Vitreoscilla.* Sp, both exhibit significant high sulfide affinities. Several factors could be responsible for these effects: Firstly, a glutamine existing at position E7 in both VHb and HbI, not commonly found in vertebrate Hbs, is involved in accelerating H_2S binding by working as an H-bond donor; Secondly, a nonpolar heme cavity consisted with three phenylalanines in HbI prevents H_2S from escaping.[16-20] Furthermore, Pluth's and Bari's groups report that the binding of H_2S to heme centre is also controlled by proximal environment such as axial ligand histidine and H-bond network.[21,22] However, it is difficult to separate the effects of distal from proximal environment on the reactivates between H_2S and heme due to the complex structure of the protein matrix which contains various modulation factors. Therefore, establishing a simple heme model with the defined structure to avoid of distal amino acids

[a] *Key Laboratory for Molecular Enzymology and Engineering of Ministry of Education, College of Life Science, Jilin University, 2699 Qianjin Street, Changchun 130012, Jilin Province, PR China. Email: lzq@jlu.edu.cn; Tel: +86-431-85155201*
[b] *Institute of Theoretical Chemistry, Jilin University, Liutiao Road 2, Changchun 130023, Jilin Province, PR China.*
[c] *National Engineering Laboratory for AIDS Vaccine, Jilin University, 2699 Qianjin Street, Changchun 130012, Jilin Province, PR China.*
[d] *Department of Physics, Georgia Southern University, Statesboro, GA 30460, USA. Email: lma@georgiasouthern.edu*
†These authors contributed equally to this work.
Electronic Supplementary Information (ESI) available: [details of any supplementary information available should be included here]. See DOI: 10.1039/x0xx00000x

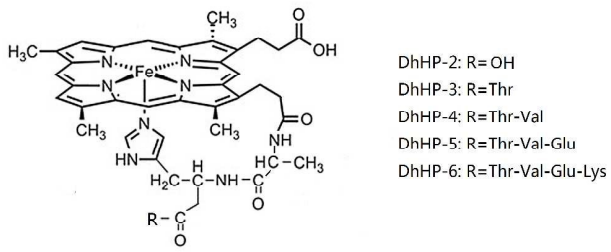

Fig. 1 Structures of deuterohemin complexes of DhHPs

is necessary for investigating the proximal mechanism of interactions between heme and H_2S.

MP-11, a heme-peptide degradated from cytochrome c proteolysis that retains the proximal histidine 18 bound to the ferric centre,[23] has been regarded as a microperoxidase and used for electrochemical,[24] spectroscopic,[25] and coordination[26] studies. Recently, this heme-peptide and other chain length derivatives are depicted as interesting models for studying the ligand binding properties of hemoproteins. In the work by Bieza et al, MP-11 has been used as a model for the investigation of the influence of the proximal environment on sulfide binding kinetics.[21] It has been reported that the reversible binding of inorganic sulfide (H_2S/HS^-) to heme-model could be attributed to two factors: i) The fifth axial ligand is essential for the formation of stable heme-H_2S/HS^- complex.[22,27] ii) The proximal hydrogen bond network affects the affinity of H_2S toward heme centre [22]. For instance, residue Thr19 in MP-11, which works as an H-bond donor, plays a key role in modulating the inorganic sulfide binding in the absence of distal effects. However, the influence of the H-bond on H_2S affinity has been studied only on the theoretical calculation level without any direct experimental results.

In this paper, to extend the comprehension of the H_2S binding kinetics modulated by proximal environment, we have synthesized a short length peptide of six amino acid residues (AlaHisThrValGluLys) referred to the residues Cys-17 to Glu-21 of MP-11. This short length peptide modified on the propionic acid side chain of deuterohemin constitutes deuterohemin-AlaHisThrValGluLys (DhHP-6). Furthermore, for exploring the effects of the axial histidine ligand in the formation of stable Fe^{III}–sulfide complex, the histidine of DhHP-6 is substituted by an alanine to obtain the derivative Deuterohemin-β-Ala-β-Ala-Thr-Val-Glu-Lys (DhAP-6). In order to further investigate the effect of the length of the peptide ''arm'' on the interaction between H_2S/HS^- and the heme iron, we have also synthesized a number of deuterohemin complexes including deuterohemin-β-Ala-His (DhHP-2), deuterohemin-β-Ala-His-Thr (DhHP-3), deuterohemin-β-Ala-His-Thr-Val (DhHP-4), and deuterohemin-β-Ala-His-Thr-Val-Glu (DhHP-5). The structures of deuterohemin derivatives are displayed in Fig. 1.

Herein, the formation of a low-spin six coordination (DhHP-6)-H_2S/HS^- complex is clearly evidenced by UV-absorption and electron paramagnetic resonance (EPR) spectroscopies, and we have evaluated the kinetics of H_2S/HS^- binding via a stopped-flow technique. We demonstrate that our DhHPs, with proximal peptide structure mimic to that in native hemeproteins, are suitable and simple heme models for evaluation of inorganic sulfide reactivity avoiding the effects of distal residues. The results to a certain extent reveal the mechanism of H_2S binding accelerated by proximal H-bond system.

Experimental

Materials

All chemicals in sample preparation were same purities as previously reported.[28] The deionized water used in all experiments was purified with a Milli-Q system (Milford, MA). Sodium sulfide nonahydrate ($Na_2S{\cdot}9H_2O$) was purchased from Sigma-Aldrich (ACS reagent, $\geqslant$ 98.0%). Fresh solution of sodium sulfide (Na_2S) was prepared in nitrogen-saturated phosphate buffered saline (PBS, 20 mM, pH 7.0) used within a day, unless otherwise stated. In all of optical absorption studies gastight Hamilton syringes were used to transfer the Na_2S solutions.

Preparation of deuterohemin derivatives

Detailed synthesis method for DhHP-6 had been published previously[28] and was adopted in this study for all deuterohemin derivative preparations. Deuterohemin was prepared following an optimized procedure.[29] Peptides (β-Ala-His, β-Ala-His-Thr, β-Ala-His-Thr-Val, β-Ala-His-Thr-Val-Glu, and β-AlaHisThrValGluLys for DhHP-2 to DhHP-6 reparations respectively and β-AlaAlaThrValGluLys for DhAP-6) were synthesized using a standard N-Fmoc/tBu solid-phase peptide synthesis protocol.[30] Briefly DCMpre-swollen Rink amide methylbenzhydrylamine (MBHA) resin. The coupling reaction was conducted when the unmodified amino acids were introduced by adding modified amino acids which were treated by Fmoc (9-Fluorenylmethoxycarbonyl). The steps (removal of Fmoc group and coupling of Fmoc-amino acid) were repeated until all amino acids in the peptide sequence and finished by synthetic coupling.

The reaction of deuterohemin to each resin coupled peptide chain was carried out in N-methylpyrrolidone (DCM). The product cleavage from the resin and removal of side chain protecting groups were carried out with a main ingredient of Trifluoroacetic acid (TFA). The crude product was washed with ether, centrifuged and dried under vacuum, then the purified products were obtained by RP-HPLC (Agilent 1200, USA) using a YMC ODS-A semi-preparative column (250×20 mm, 10 μm YMC Co., Ltd. Japan). Analytical RP-HPLC and MALDI-TOF-MS/MS (AB SCIEX, USA) were used to confirm the purity and molecular weight of DhHP-2, -3, -4, -5, and -6 as well as DhAP-6. The purity was confirmed to be greater than 98.5% for all deuterohemin derivatives. Mass spectra were shown in Fig. S1 and experimental molecular weights compared with calculated were listed in Table. S1 of the supplementary materials.

Spectroscopic methods

Deuterohemin derivatives were dissolved in PBS and all buffers were purged with nitrogen gas before use. A stock solution of 2 mM Na_2S was prepared in 100 mM succinic acid buffer in an anaerobic chamber (MiniMacs Anaerobic Workstation, Don Whitley Scientific Ltd., Shipley, UK). The binding reactions were carried out by adding 10 µL of degassed Na_2S stock solution into 1 mL of DhHP-6 or DhAP-6 sample (~ 5 µM) to a final sulfide concentration of 20 µM (4 molar eq. ratio to deuterohemin-peptides).

The UV–visible spectra before and after sulfide binding reactions were recorded in a 1-cm cuvette using a UV-2700 spectrophotometer system (Shimadzu, Japan) equipped with a temperature controller at 25 ℃. The spectra were collected over 300 –700 nm at 600 nm/min with a data point interval of 0.5 nm for all samples.

EPR measurements were performed using a Bruker EMXplus X-band spectrometer equipped with ColdEdge CH-210N Cryocooler at 15 K in a quartz tube (2 mm i.d., 1 mm thickness (Technical Glass Products, Inc.). The sulfide stock solution was added to DhHP-6 or DhAP-6 sample (400 µM) at different ratios of molar equivalent. The reaction was terminated at desired time in liquid nitrogen before the measurement. Spectra were recorded under the following EPR conditions: centrefield, 2500 G; scan range, 5000 G; field modulation, 1.0 G; microwave power, 2 mW; time constant, 0.1 s; and scan time, 4 min.

Kinetic Measurements

The sulfide association rate constants were determined using a stopped-flow rapid scanning spectrophotometer (Applied Photophysics, Leatherhead, UK) under pseudo-first-order conditions. Briefly, solution of DhHPs (10 µM, 100 µL) was mixed rapidly with an equal volume of Na_2S solution at different concentrations ranging from 0.25 to 2 mM. H_2S/HS^- concentration before the reaction was confirmed from the absorbance at 230 nm (molar absorptivity = 7200 $M^{-1}cm^{-1}$) as described previously.[18, 21] The reaction was monitored for 0.25 s (the dead time of 1 ms) through DhHP-H_2S/HS^- absorbance increasing at 407 nm, the maximum in the static absorption spectrum of the DhHP-H_2S/HS^- shown in Fig. 2A. All other derivatives were measured under the same pseudo-first-order condition. The apparent rate constants (k_{obs}) were obtained by curve fitting association traces into single exponential functions.[16] The second-order rate constants (k_{on}) were calculated from the k_{obs} values versus the sulfide concentrations. Each reaction was duplicated three times independently. The sulfide dissociation rate constants (k_{off}) of DhHPs were measured by a imidazole ligand replacement method using a stopped-flow technique as described previously.[21, 31] Briefly, DhHP-H_2S/HS^- complexes were mixed rapidly with imidazole in PBS at concentration ratios of [imidazole]/ [DhHP-H_2S/HS^-] range from 100:1 to 1000:1. The reactions were followed by the increase of the absorbance at 399 nm, a characteristic absorption of the formation of DhHP-imidazole complex (see Fig. 2C). Under this condition, k_{obs} of the displacement trace equals to k_{off} due to [imidazole] >> [sulfide].[21, 31]

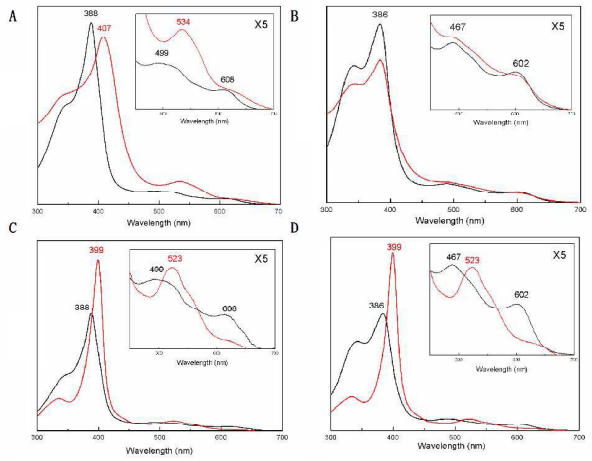

Fig. 2 (A) UV–vis spectra of ferric DhHP-6 in the absence of H_2S/HS^- (black) and after addition of H_2S/HS^- (red); (B) UV–vis spectra of ferric DhAP-6 in the absence of H_2S/HS^- (black) and after addition of H_2S/HS^- (red). Condition for (A) and (B): DhHP-6/DhAP-6 at 5 µM reacted with 20 µM Na_2S in degassed PBS at pH 7.0 and 25 ℃ for 2 min. (C) UV–vis spectra of DhHP-6 in the absence (black) or presence of imidazole (red);. (D) UV–vis spectra of DhAP-6 in the absence (black) or presence of imidazole (red). Condition for (C) and (D): 5 µM DhHP-6/DhAP-6 reacted with 5 mM imidazole in degassed PBS at pH 7.0 and 25 ℃ for 2 min.

Results and discussion

Spectroscopic Characterization

Fig. 2 depicts the static absorption spectra recorded before and after the addition of Na_2S solution (4 eq.) to deoxygenated solutions of DhHP-6 (Fig. 2A) and DhAP-6 (Fig. 2B). In the absence of Na_2S solution, the absorption spectra of DhHP-6 and DhAP-6 (black lines) are characterized by strong soret band absorption maximum at 388 nm and 386 nm, respectively. The addition of Na_2S results in the formation of (DhHP-6)-H_2S/HS^- complex (red line), which is clearly evidenced by the red shift of the Soret band from 388 nm to 407 nm in Fig. 2A. Simultaneously, the principle Q-band absorbance at 499 nm and 608 nm disappear with the associated formation of a new absorption at 534 nm. Similar spectroscopic changes have been previously observed in the binding of H_2S/HS^- to ferric MP-11 and met-hemCD3.[21,27] By contrast, it has been reported that synthetic picket-fence porphyrins[27] and a haemoglobin model which does not possess the axial nitrogenous ligand[22] do not coordinate with sulfide but are reduced to the ferrous species. Thus, the absorption intensity dropping in DhAP-6 after addition of sulfide for 2 min (Fig. 2B) and the Soret band red-shifting 10 min after the reaction (Fig. S2) may be due to the reduction of the ferric to ferrous species. The direct evidences for the reduction are provided in our EPR data. To further investigate the role of proximal histidine in sulfide binding reactions imidazole solution (5 mM in PBS) has been added into DhHP-6 and DhAP-6.

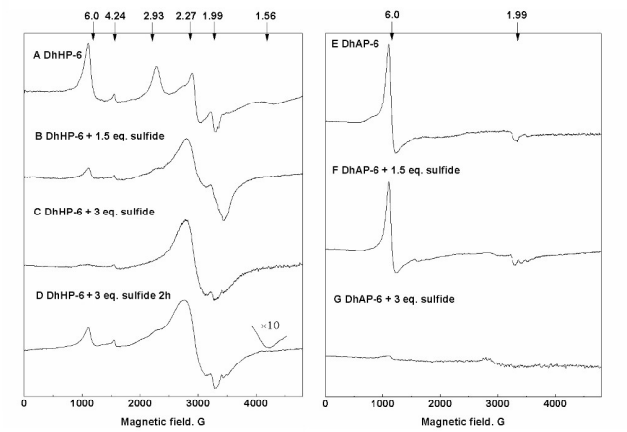

Fig. 3 EPR spectra of (A) DhHP-6 (4.0×10^{-4} M) in the absence H_2S/HS^-, (B) DhHP-6 in the presence of H_2S/HS^- (1.5 eq.) after 5 min, (C) DhHP-6 in the presence of H_2S/HS^- (3 eq.) after 5min, (D) DhHP-6 in the presence of H_2S/HS^- (3 eq.) after 2 hour (E) DhAP-6 (4.0×10^{-4} M) in the absence H_2S/HS^-, (F) DhAP-6 in the presence of H_2S/HS^- (1.5 eq.) and (G) DhAP-6 in the presence of H_2S/HS^- (3 eq.). All the spectra were measured in PBS at pH 7.0 and 15 K.

Both samples shift their Soret absorption bands from 388 and 386 nm to 399 nm respectively (Fig. 2C and 2D). It appears that differently from typical ligands such as imidazole and CN^-, inorganic sulfide does need proximal ligand histidine to control the binding to ferric hemes.

Fig. 3 depicts the EPR spectra recorded before and after the reaction of DhHP-6 with H_2S/HS^-. In absence of Na_2S, DhHP-6 (Fig. 3A) reveals three features: (1) EPR signals with the lowest g value at 1.99 and the highest g at 6.00 are from the |±1/2> doublet of high spin (HS) S = 5/2 ferric centre with E/D ≈ 0.00, (2) a very weak rhombic HS signal with g value at 4.24 is due to |±3/2> doublet with E/D ≈ 0.33, [32] and (3) a low spin (LS) ferric centre has g values of 2.93, 2.27, and 1.56. In terms of HS signals, it is a typical signature of five coordination of heme-proteins or models, indicating the existence of the two HS species with different rhombicities.[32] On the other hand, the LS signals around g = 2 region are interpreted as a LS rhombic type II ferric species[33] which can be attributed to the intra interaction of Lys at the end of six-amino-acid chain in DhHP-6 with its ferric centre through the 6th coordination position.[34] The similar g values were observed in microperoxidase MP-9 at pH 7. After adding H_2S/HS^- at 1.5 eq. ratio, the high-spin EPR decreased dramatically in very short time (Fig. 3B). As the ratio increased to 3 eq. the HS EPR peaks completely vanished (Fig. 3C) in 5 min. At the same time, the LS characteristics were totally replaced by a more isotropic LS EPR signal as the rhombic signal at g_{max} of 2.93 and g_{min} of 1.56 disappeared. The new isotropic EPR could be ascribed to the formation of a six-coordinated low-spin Fe^{III}-H_2S/HS^- complex. It had been observed that LS g values moved towards to the centre g value in human ferric sulf-Hb when changing ligand from CN^- to SH^-, resulting in a change of g_{max} from 2.74 to 2.36 as well as g_{min} from 1.65 to 1.93.[35] The characteristic peaks of HS DhHP-6 at g = 6.00 and LS at g_{max} = 2.93 and g_{min} = 1.56 recovered after 2 hours of the reaction (Fig. 3D), which indicated the partial escape of bound H_2S/HS^- and the reversibility of the binding reaction. In contrast, the EPR spectrum of DhAP-6 shows no low spin EPR signal upon addition of sulfide at 1.5 eq. ratio (Fig. 3F) and similar to that before the reaction (Fig. 3E). When increasing H_2S/HS^- concentration to 3 eq. ratio, the high spin EPR signal has completely disappeared (Fig. 3G) indicating the formation of the ferrous from sulfide reduced ferric species. These results reveal that the axial histidine ligand is the key factor to stabilize ferric iron for the formation of a stale Fe^{III}-H_2S/HS^- complex (Scheme 1A), which is consistent with the previous reported results.[27]

Kinetics

It has been believed that the Gln at E7 position, involved in distal heme pocket hydrogen bond network,[16,19,20] could be responsible for the high sulfide reactivates towards to VHb[19] and HbI[17]. To investigate if the proximal environments also affect H_2S/HS^- binding reaction, we have tested a series of DhHP-2 to -6 without distal structures in this study. Fig. 4A shows three representative sulfide association traces of DhHP-2, -3 and -6 and Fig. 4B plots the observed rate constants k_{obs} of DhHP-2 to -6 obtained by fitting the traces to exponential functions as y-axis and the sulfide concentrations as x-axis. It is obvious that k_{obs} constants are linearly dependent on the sulfide concentrations for the ratios of [sulfide]/[DhHP]

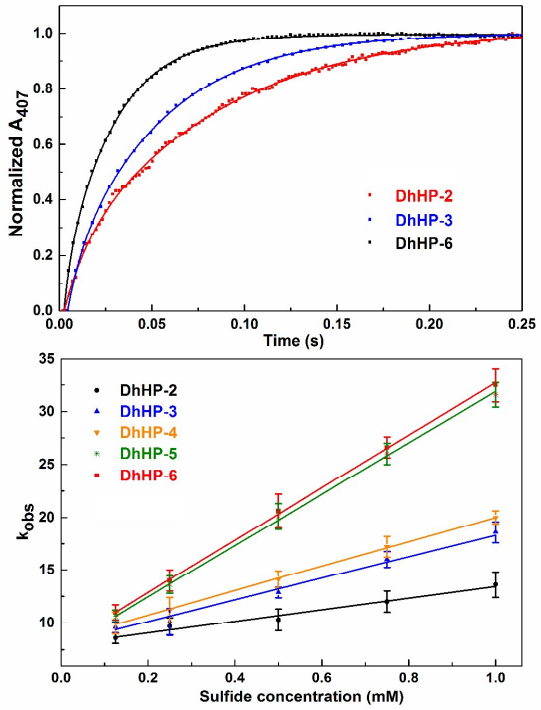

Fig. 4 (A) Exponential sulfide association traces of 5 μM DhHP-2, DhHP-3 and DhHP-6 (with 500 μM Na_2S in PBS at pH 7.0 and 25 °C during 0.25 s. (B) Plots of k_{obs} as functions of H_2S concentrations for DhHP-2, -3, -4, -5 and -6 samples.

ranging from 10:1 to 100:1 (corresponding to sulfide final concentrations of 125 μM to 1000 μM). The values of association rate constant, k_{on}, are calculated from the slopes of the plots in Fig. 4B and summarized in Table 1. DhHP-6 exhibits the fastest second-order association rate constant with k_{on}= 2.34 ×10^4 $M^{-1}s^{-1}$ and the rate is similar to those of MP-11,[21] Bs-trHb and HbII/III from *Lucina pectinata*.[17, 21] Even though k_{on} of DhHP-6 is one order of magnitude lower than those of VHb[19] and HbI,[17] our results indicate that there are proximal factors controlling the binding of sulfide towards ferric heme beside the effects of distal heme pocket environment. The binding may be governed by proximal environment especially proximal H-bond network. The hypothesis can be tested by alerting amino acid residues around ferric centre in proximal direction. As shown the structures of DhHPs in Fig. 1, DhHP-3 and -4 have one Thr3 residue and DhHP-5 and -6 have both Thr3 and Glu5. While DhHP-2 (Ala-His) has none of them and, as expected, exhibits the slowest association rate constant, k_{on} = 0.58×10^4 $M^{-1}s^{-1}$. Accordingly, the k_{on} values of DhHP-3 and -4 are close and about 2 times higher, while the values of DhHP-5 and -6 are about 4 times higher than that of DhHP-2. Clearly, the k_{on} substantially increases by introducing Glu at position 5 in DhHP-5 and -6 indicates that it is suitable residue to provide H-bond due to its appropriate orientation and position. No significant difference of k_{on} is observed between DhHP-5 (Ala-His-Thr-Val-Glu) and DhHP-6 (Ala-His-Thr-Val-Glu-Lys), demonstrating that Lys at position 6 may not be crucial for H_2S/HS^- reactivity. Likewise, DhHP-3 and -4 shows similar values of k_{on}, which indicates that Val4, an amino acid incapable to be involved in H-bond, may be less effective on the binging. These results are confirmed by our theoretical calculations provided in Supplementary Information (Fig. S3). The increase of Mulliken atomic charges (Fe^{III}) follows the same trend with the increases of k_{on} from DhHP-2 to -6. Since the peptide chain of the DhHP-6 is mimetic models of proteolysis of cytochrome c as described above, our results could reveal that the proximal ligand His and H-bond network are essential for the inorganic sulfide binding in the case of native sulfide-reactive heme-containing protein in vivo.

The ligand-displacement process of (DhHP-6)-H_2S/HS^- is shown in Fig. 5 by following the increasing of the characteristic absorption of DhHP-imidazole complex at 399 nm with time. DhHP-6Fe^{III}-H_2S/HS^- dissociation rate constant, k_{off}, has been calculated from the apparent rate constant k_{obs} obtained by fitting the DhHP-imidazole formation curve in Fig. 5 inset to an exponential rise function, assuming $k_{off} \approx k_{obs}$ since the concentration of the ligand imidazole is much higher than Na_2S concentration. Using same method, all values of k_{off} for DhHP-2 to -6 are obtained and listed in Table. 1. DhHP-6 exhibits a dissociation rate constant, k_{off} = 7.2 s^{-1}, close to that of MP-11 (k_{off}= 5.7 s^{-1}). In addition, no systemic change of k_{off} values is observed for all DhHPs-sulfide complexes when the length of the peptide chain changed from 2 to 6 residues. We conclude that, in contrast to the case of k_{on}, the proximal environment does not affect k_{off} much. In fact, the values of k_{off} of DhHPs in this study as well as MP-11 are four orders of magnitude higher than that of native HbI and VHb[17, 19], which may be due to lack of distal blocking structure in the mimetic models. Furthermore, the k_{off} values exhibit sharp differences between diverse heme-containing proteins, for instance, HbII/III with different distal environments, exhibit a 10-fold higher k_{off} than that of HbI (k_{off} = 2.2×10^{-4}). It has been reported that there are some barriers governing the stabilization of the bound H_2S/HS^- such as bulkier amino acid residues at distal heme pocket and transient fluctuations of the protein.[16] For instance, a non-polar cavity exist in HbI consists of three phenylalanines availably prevented bound H_2S from escaping. The lack of the

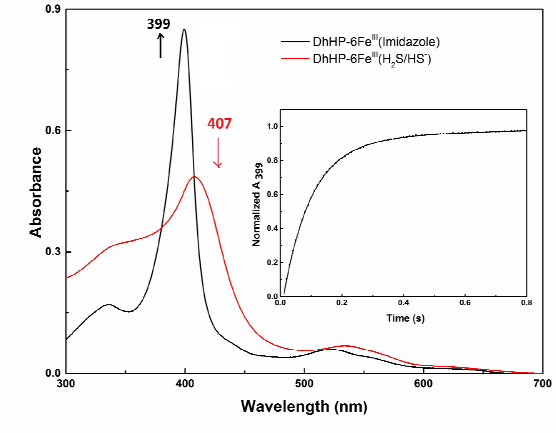

Fig. 5 UV-Vis spectra of DhHP-6-sulfide complex (red) and after sulfide replacement reaction (black) at the ratio of [imidazole] / [H_2S] of 1000:1. Insert: Kinetic trace at 399 nm. Under this condition the observed rate for displacement of H_2S by imidazole equals to k_{off}.

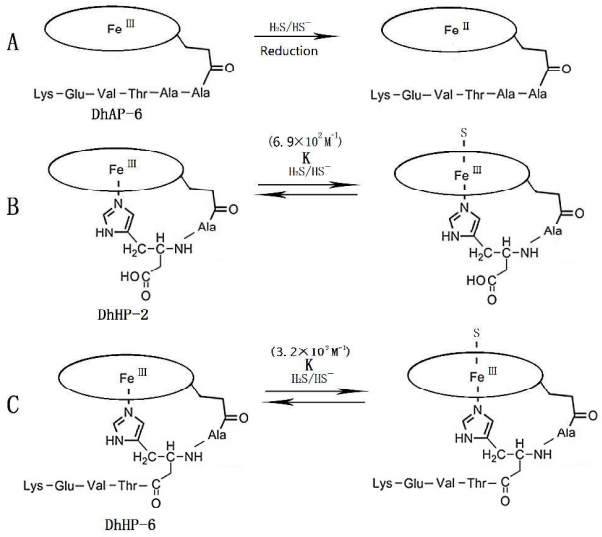

Scheme 1 Reactivity of deuterohemin complexes with H_2S/HS^-.

Table. 1 Association and dissociation rates constants for binding of H_2S/HS^- to heme-peptides, Hbs from invertebrates and VHb.

Sample	k_{on} ($\times 10^4$ $M^{-1}s^{-1}$)	k_{off} (s^{-1})	K(M^{-1})
DhHP-2	0.58	8.5	689
DhHP-3	1.1	8.2	1305
DhHP-4	1.18	8.8	1307
DhHP-5	2.31	7.5	3040
DhHP-6	2.34	7.2	3208
MP-11[a]	2.60	5.7	4561
Hbl[b]	23	2.2×10^{-4}	1.0×10^{9}
VHb[c]	12	2.5×10^{-4}	4.8×10^{8}

[a] *Data taken from reference [21],*
[b] *Data taken from reference [17],*
[c] *Data taken from reference [19].*

distal protein structure is responsible for the high values of k_{off} for heme-peptide models. Finally, the last column of Table 1 shows the formation constants, K, calculated from the ratio of k_{on}/k_{off}. The values of K increased nearly five-folds with the increase of the peptide length from 2 to 6 (Scheme. 1B and 1C). We demonstrated that proximal H-bond network is an essential factor for modulating the affinity between H_2S/HS^- towards heme centre.

Conclusions

To investigate the effect of proximal environment on sulfide binding a series of deuterohemin complexes are constructed, providing heme peptide models in absence of distal stabilization mechanisms. UV-Vis and EPR spectroscopies are used to confirm the binding reactions. The formation of new low-spin and the disappearance of high spin species when DhHP-6 reacts with inorganic sulfide reveal the reactive capability of its ferric center. Kinetic parameters of the association and dissociation reactions are determined by Soret band shifting in DhHP-2, -3, -4, -5 and -6 samples under physiological condition. The results indicate that the introduction of Glu5, in the case of DhHP-5 and -6, enhances the sulfide association reaction. The enhancement suggests that the proximal hydrogen bond network facilitate the sulfide binding. When replacing His2 with Ala2 it has been observed that ferric can be easily reduced to ferrous by sulfide in DhAP-6, indicating that the proximal histidine plays a key role to resist the heme center reduction.

Acknowledgements

The authors are grateful for the financial support from the National High Technology Research and Development Program of China ("863"Program, 2012AA022202B).

Notes and references

1 S. Bo, *Biochim. Biophys. Acta*, 1958, **27**, 324-329.
2 P. Nicholls and J. K. Kim, *Can. J. Chem.*, 1982, **60**, 613-623.
3 J. A. Strickland and G. L. Foureman, *Sci Total Environ.*, 2002, **288**, 51-63.
4 L. Li, . and P. K. Moore, *Biochem. Soc. Trans.*, 2007, **35**, 1138-1141.
5 L. Li and P. K. Moore, *Trends Pharmacol. Sci.,* 2008, **29**, 84-90.
6 K. Kashfi and K. R. Olson, *Biochem. Pharmacol.*, 2013, **85**, 689–703.
7 K. Hideo, S. Norihiro and K. Yuka, *Antioxidants & Redox Signaling*, 2012, **17**, 45-57.
8 K. Omer and B. Ruma, *J. Biol. Chem.*, 2010, **285**, 21903-21907.
9 K. Mayumi, F. Ryo, R. M. Bateman, Y. Takehiro and S. Makoto, *Antioxidants & Redox Signaling*, 2009, 13(2): 157-92
10 G. A. Benavides, G. L. Squadrito, R. W. Mills, H. D. Patel, I. T Scott, R. P. Patel, V. M. Darley-Usmar, J. E. Doeller and D. W. Kraus, *Proceedings of the National Academy of Sciences*, 2007, **104**, 17977-17982.
11 H. Kimura, *Antioxidants & Redox Signaling*, 2010, **12**, 1111-1123.
12 X. Huang and S. G. Boxer, *Nat. Struct. Biol*., 1994, **1**, 226-229.
13 T. Sugimoto, M. Unno, Y. Shiro, Y. Dou and M. Ikeda-Saito, *Biophys. J* ., 1998, **75**, 2188-2194.
14 R. Pietri, R. G. León, L. Kiger, M. C. Marden, L. B. Granell, C. L. Cadilla and J. López-Garriga, *Biochim. Biophys. Acta -Proteins and Proteomics*, 2006, **1764**, 758-765.
15 M. D. Salter, K. Nienhaus, G. U. Nienhaus, S. Dewilde, L. Moens, A. Pesce, M. Nardini, M. Bolognesi and J. S. Olson, *J. Biol. Chem.*, 2008, **283**, 35689-35702.
16 P. Ruth, A. Lewis, R. G. León, G. Casabona, L. Kiger, Y. S. Ru, S. F. Alberti, M. C. Marden, C. L. Cadilla and G. L. J., *Biochemistry*, 2009, **48**, 4881-4894.
17 D. W. Kraus and J. B. Wittenberg, *J. Biol. Chem.*, 1990, **265**, 16043-16053.
18 (a) M. N. Hughes, M. N. Centelles, K. P. Moore, *Free Radical Biol. Med.* 2009, 47, 1346–1353. (b) P. Nagy, Z. Pálinkás, A, Nagy, B. Budai, I. Tóth, A, Vasas. *Biochim Biophys Acta.* 2014,1840(2):876-91.
19 D. Wang, L. Liu, H. Wang, H. Xu, L. Chen, L. Ma and Z. Li, *FEBS Lett.*, 590 (2016) 1132–1142.
20 C. R. Alvarez, B. K. Yoo, R. Pietri, I. Lamarre, J.-L. Martin, J. Lopez-Garriga and M. Negrerie, *Biochemistry*, 2013, **52**, 7007-7021.
21 S. A. Bieza, F. Boubeta, A. Feis, G. Smulevich, D. A. Estrin, L. Boechi, and S. E. Bari, *Inorganic Chemistry*, 2015, **54**, 527-533.
22 M. D. Hartle, J. S. Prell and M. D. Pluth, *J. Chem. Soc., Dalton Trans.*, 2016, **45**, 4843-4853.
23 A. Spector, W. Zhou, W. Ma, C. F. Chignell and K. J. Reszka, *Experimental eye research*, 2000, **71**, 183-194.
24 H. M. Marques, *Inorg. Chem.*, 1990, **29**, 1597-1599.
25 J. W. Owens and C. J. O'Connor, *Coord. Chem. Rev.*, 1988, **84**, 1-45.
26 M. S. Hamza and J. Pratt, *J. Chem. Soc., Dalton Trans.*, 1994, 1367-1371.

27 K. Watanabe, T. Suzuki, H. Kitagishi and K. Kano, *J. Chem. Soc., Chem. Commun.*, 2015, **51**, 4059-4061.
28 Q. G. Dong, Y. Zhang, M. S. Wang, J. Feng, H. H. Zhang, Y. G. Wu, T. J. Gu, X. H. Yu, C. L. Jiang and Y. Chen, *Amino Acids*, 2012, **43**, 2431-2441.
29 W. S. Caughey, J. O. Alben, W. Y. Fujimoto and J. L. York, *J. Org. Chem.*, 1966, **31**, 2631-2640.
30 C. J. Palestro, F. L. Weiland, J. E. Seabold, S. Valdivia, M. B. Tomas, B. R. Moyer, Y. M. Baran, J. Lister-James and R. T. Dean, *Nuclear Medicine Communications*, 2001, **22**, 695-701.
31 I. Birukou, R. L. Schweers and J. S. Olson, *J. Biol. Chem.*, 2010, **285**, 8840-8854.
32 W. R. Hagen, *J. Chem. Soc., Dalton Trans.*, 2006, 4415-4434.
33 G. Zoppellaro, K. L. Bren, A. A. Ensign, E. Harbitz, R. Kaur, H. P. Hersleth, U. Ryde, L. Hederstedt and K. K. Andersson, *Biopolymers*, 2009, **91**, 1064-1082.
34 A. Riposati, T. Prieto, C. S. Shida, I. L. Nantes and O. R. Nascimento, *J. Inorg. Biochem.*, 2006, **100**, 226-238.
35 N. L. Bafus, S. C. Albright, R. D. Todd and W. T. Garrard, *J. Biol. Chem.*, 1978, **253**, 2568-2574.